

# Edge and bulk transport in the mixed state of a type-II superconductor

Z. L. Xiao and E. Y. Andrei

*Department of Physics and Astronomy, Rutgers University, Piscataway, New Jersey 08855*

Y. Paltiel and E. Zeldov

*Department of Condensed Matter Physics, The Weizmann Institute of Science, Rehovot 76100, Israel*

P. Shuk and M. Greenblatt

*Department of Chemistry, Rutgers University, Piscataway, New Jersey 08854*

(Received 17 August 2001; published 13 February 2002)

By comparing the voltage-current ( $V$ - $I$ ) curves obtained before and after cutting a sample of  $2\text{H-NbSe}_2$ , we separate the bulk and edge contributions to the transport current at various dissipation levels and derive their respective  $V$ - $I$  curves and critical currents. We find that the edge contribution is thermally activated across a current dependent surface barrier. By contrast the bulk  $V$ - $I$  curves are linear, as expected from the free flux flow model. The relative importance of bulk and edge contributions is found to depend on dissipation level and sample dimensions. We further show that the peak effect is a sharp bulk phenomenon and that it is broadened by the edge contribution.

DOI: 10.1103/PhysRevB.65.094511

PACS number(s): 74.25.Fy, 74.60.Ec, 74.60.Ge, 74.60.Jg

## I. INTRODUCTION

One of the remarkable differences between a normal metal and a superconductor stems from the way they carry current. While in metallic samples the current density is usually homogeneous throughout the material, in superconductors in the Meissner state the current flows along the sample surface and edges so as to eliminate the self-induced magnetic field within the sample volume. In type-II superconductors in the mixed state, where the material is permeated by magnetic flux lines (vortices), a similar current enhancement along sample edges is the result of a surface barrier which inhibits the entry or exit of vortices.<sup>1-13</sup> Several types of surface barriers have been identified including the Bean-Livingston<sup>1</sup> and geometrical<sup>2,3</sup> barriers. The former, which is the primary source of edge currents in the experiments described here, is a result of the competition between the attraction of a vortex to its image and the repulsion arising from its interaction with shielding currents. Recent Hall probe measurements in  $\text{Bi}_2\text{Sr}_2\text{CaCu}_2\text{O}_8$  (Refs. 4-6) and  $\text{NbSe}_2$  (Ref. 7) crystals have shown edge current enhancement due to the surface barrier. But thus far these edge currents were only qualitatively identified.

The experiments described here allow for the first time to derive individual voltage-current ( $V$ - $I$ ) characteristics of the edge and bulk currents. Below the peak effect region (a peak in the critical current just below  $T_c$ ) we find that vortex entry and exit at the edges is governed by thermal activation across a current dependent surface barrier, whereas vortex motion in the bulk is nonactivated. Our results show that the observed nonlinearities of the  $V$ - $I$  characteristics are due to the edge contribution while the bulk  $V$ - $I$  curves are linear. We further show that the peak in critical current is primarily a bulk effect which sharpens and becomes more pronounced when the edge contribution is removed. These experiments demonstrate that boundaries have a profound effect on the  $V$ - $I$  char-

acteristics as well as on the field and temperature dependence of the critical current.

## II. EXPERIMENTAL DETAILS

The experiments were carried out in the low temperature superconductor  $2\text{H-NbSe}_2$  where local self-field<sup>7</sup> and magnetization<sup>13</sup> measurements unveiled the presence of significant edge currents. Transport, neutron scattering and magnetization measurements in these samples<sup>14-26</sup> revealed a number of unusual phenomena including memory and current driven reorganization.<sup>16-24</sup> In addition, the shape of the peak effect in this material was found to change significantly with measurement speed<sup>20,24</sup> or contact configuration.<sup>25</sup> Several of these results were shown to be a consequence of vortices traversing a surface barrier as they enter the sample.<sup>24,25</sup> In the experiments described here the surface barrier was determined after separating the edge and bulk contributions to the current. The separation procedure involves cutting a sample to reduce its width and comparing the  $V$ - $I$  characteristics before and after cutting. A schematic illustration of the cutting is given in Fig. 1(a).

The data were acquired on two undoped single crystals of  $2\text{H-NbSe}_2$  with initial sizes of  $8(L) \times 1.72(w) \times 0.020(d)$  mm<sup>3</sup> (sample A) and  $6.3(L) \times 1.40(w) \times 0.060(d)$  mm<sup>3</sup> (sample B) and with zero field critical temperatures and width of  $T_c = 7.18$  K,  $\Delta T_c = 95$  mK and 7.21 K, 92 mK, respectively. Our measurements employed a standard four probe technique with low resistance  $\text{Ag}_{0.1}\text{In}_{0.9}$  solder contacts. The distance between the voltage contacts was 2.5 and 1.5 mm in samples A and B, respectively. The critical current,  $I_c$ , is defined as the current at which the voltage reaches  $1 \mu\text{V}$ . The magnetic field was kept along the  $c$  axis of the sample and the dc current was applied in the  $a$ - $b$  plane. The vortex lattices are prepared by applying the magnetic field after cooling the sample through  $T_c$  (zero-field cooling). Sample cut was carried out manually with a

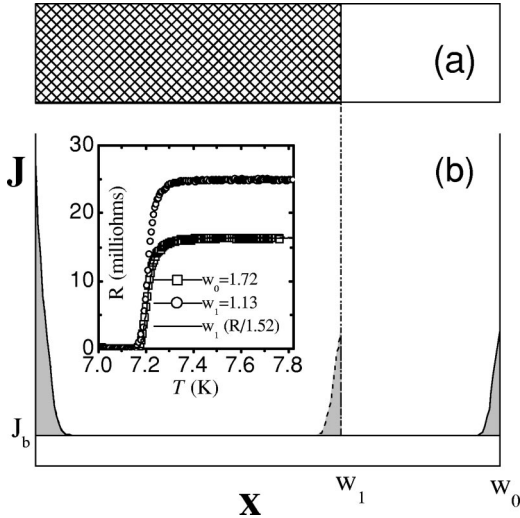


FIG. 1. Schematic illustrations of sample cutting (a) and the corresponding current distributions in the vortex state (b). The shaded area represents the edge current  $I_s$  (see text). The inset in (b) shows the resistance versus temperature curves and the determination of the ratio of the sample width before ( $w_0$ ) and after ( $w_1$ ) cutting.

sharp razor blade. The width reduction factor  $\alpha_{0n} = w_0/w_n$  ( $w_0$ ,  $w_n$  are the width before and after  $n$ th cutting) was determined by direct inspection under a microscope and confirmed by measuring the ratio of normal state resistances before and after cutting. Sample A was cut twice with  $\alpha_{01} = 1.52$  [shown in the inset of Fig. 1(b)] and  $\alpha_{02} = 3.65$  for the first and second cuts, respectively, and sample B was cut once with  $\alpha_{01} = 1.35$ . By using this procedure rather than samples with different widths one can be certain that in comparing the  $V$ - $I$  curves before and after cutting all the parameters (excepting the newly cut edge) are the same.

### III. RESULTS AND DISCUSSION

In Fig. 2 we show the effect of sample cutting by comparing the  $V$ - $I$  curves and critical currents before and after cutting. In Fig. 2(a) the results are shown for both the normal ( $T = 7.6$  K  $> T_c$ ) and superconducting ( $T = 4.25$  K  $< T_c$ ) states at  $H = 1$  T. A comparison of the measurements at the same average current density ( $J = I/dw$ ) is obtained by plotting the voltage against the scaled current  $\alpha_{02}I$  (solid line). At 7.6 K the scaled curve exactly overlaps the response in the uncut sample, clearly showing that the current density in the normal state scales with the inverse of the sample width. In other words the current distribution in the normal state is uniform. Using the same procedure for the data in the vortex state, we find that the scaled  $V$ - $I$  curve of the cut sample is shifted to the right of the initial curve, indicating that for the same voltage response the average current density in the cut sample is much higher. The same tendency is found for the scaled critical currents, which are significantly larger after cutting, Fig. 2(b). As shown below these results are consistent with an enhanced current at the sample edges due to the surface barrier. In fact both theories<sup>1,10,11</sup> and experiments<sup>4-7,12,13</sup> favor an excess current carrying capacity

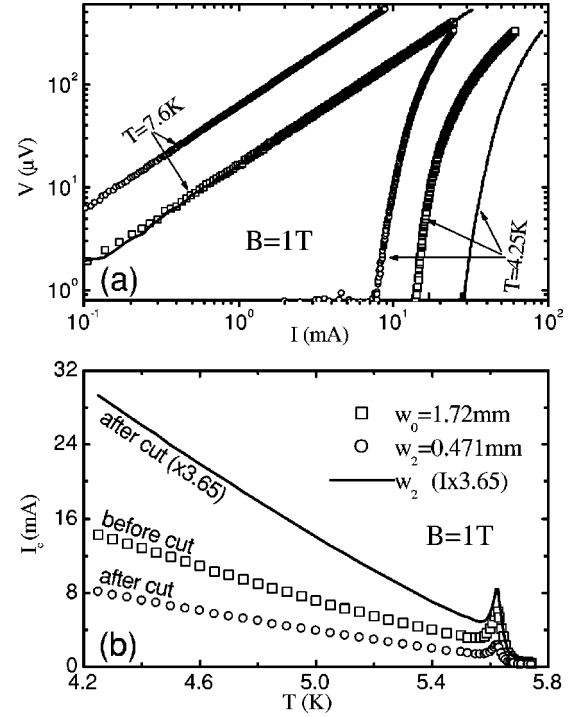


FIG. 2.  $V$ - $I$  curves at temperatures below (4.25 K) and above (7.60 K) the critical temperature  $T_c$  (a) and temperature dependence of critical current (b) for sample A before and after sample cutting. The open symbols and solid lines represent the as-measured and the scaled data.

at the sample edges. The results are analyzed by separating the total current  $I = I_s + I_b$  into a uniformly distributed bulk contribution  $I_b = J_b w d$ , with current density  $J_b$  and a nonuniform contribution  $I_s$ . The latter, assumed to remain unchanged after cutting, represents the edge current due to the surface barrier.<sup>1-3</sup> If edge contamination<sup>24</sup> is present the resulting enhanced edge current would also be included in  $I_s$ . This model is applicable when the sample width after cutting is much larger than the characteristic extent of edge currents. In our experiments this condition is well satisfied below the peak effect regime where edge currents are predominantly due to the surface barrier (edge contamination is negligible<sup>24</sup>) and are thus confined to within a narrow strip  $\leq \lambda \sim 100$  nm  $\ll w$ .<sup>10,11</sup> It follows that the vortex velocity and hence the voltage response at a given field and temperature is uniquely determined by the bulk current density  $J_b$  and by  $I_s$ . In Fig. 1(b) we plot a schematic current distribution in the presence of a surface barrier<sup>1,10,11</sup> or/and edge contamination illustrating the effect of cutting for a constant  $J_b$ . In this model the voltage response to a driving current  $I = I_b + I_s$  in the initial sample will be the same as the response to a current  $I_\alpha = I_b/\alpha + I_s$  in the cut sample, leading to a straightforward procedure for analyzing the data and for separating bulk from surface currents. Thus, after obtaining the values of  $I$  and  $I_\alpha$  at a given voltage response by measuring the  $V$ - $I$  curves before and after cutting the sample, the bulk and surface contributions to the current are given by  $I_b = \alpha(I - I_\alpha)/(\alpha - 1)$  and  $I_s = (\alpha I_\alpha - I)/(\alpha - 1)$ . Repeating the same procedure for various voltage levels, separate  $V$ - $I$

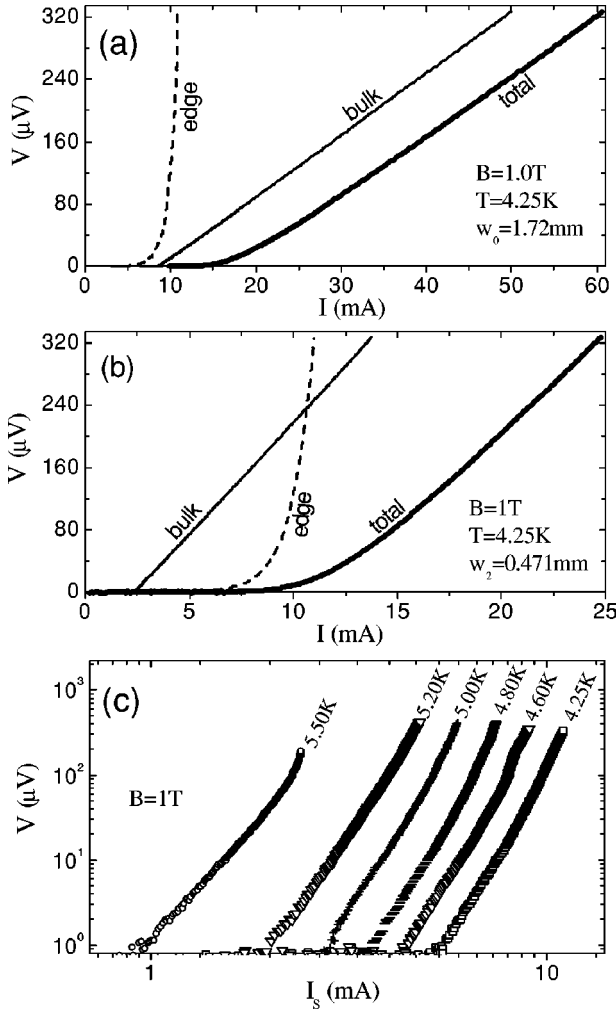


FIG. 3.  $V$ - $I$  curves for total (thick line), edge (dashed), and bulk (thin line) current before (a) and after (b) cutting the sample. (c) edge  $V$ - $I_s$  curves in 1 T and at various temperatures.

characteristics can be obtained for the bulk ( $V$ - $I_b$ ) and the edge ( $V$ - $I_s$ ). Results for the  $V$ - $I$  characteristics of sample A at 4.25 K and 1 T are shown in Figs. 3(a) and 3(b) for the initial ( $w_0 = 1.72$  mm) and cut sample ( $w_2 = 0.471$  mm), respectively. We note that the relative contribution of the edge is larger in the narrower sample Fig. 3(b) than in the wider one Fig. 3(a), in accord with the assumption that  $I_s$  is unchanged, whereas  $I_b$  is proportional to the sample width. In addition, the relative contribution of the edge to the total transport current diminishes with increasing dissipation level indicating that the voltage grows much faster with increasing  $I_s$  than it does with  $I_b$ . We further note that the measured  $V$ - $I$  curves in both the initial and cut samples are nonlinear at modest dissipation levels. Previous interpretations of the nonlinearities in the  $V$ - $I$  curves in 2H-NbSe<sub>2</sub> were usually based on the assumption of a bulk phenomenon. However from Figs. 3(a) and 3(b), our data show that the nonlinearity is due to the edge contribution whereas the bulk  $V$ - $I$  curves are remarkably linear, consistent with early models of vortex motion in low temperature superconductors.<sup>27,28</sup>

Theoretical studies of vortex entry and exit across sample

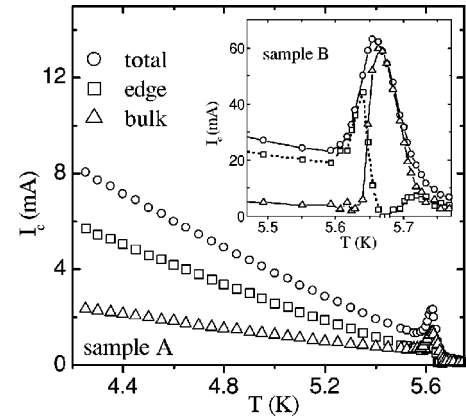


FIG. 4. Temperature dependence of total, edge and bulk critical currents at 1 T. Main panel: results for sample A ( $w_2 = 0.471$  mm); inset: expanded view of the peak region for sample B ( $w_0 = 1.40$  mm).

edges<sup>10,11</sup> have shown that a surface barrier  $U(I_s)$ , gives rise to thermally activated  $V$ - $I_s$  characteristics:  $V = V_0 \exp[-U(I_s)/k_B T]$ . The current dependence of the surface barrier is determined by the mechanism of vortex penetration. For example, the surface barrier in a slab geometry was found to have a power law current dependence  $U \sim I_s^{-1/2}$  in the 3D case while in the 2D case it is logarithmic  $U \sim U_0 \ln(I_0/I_s)^{1/2}$  with  $U_0$  a characteristic energy scale.<sup>10,11</sup> In Fig. 3(c) we plot the edge  $V$ - $I_s$  characteristics at 1 T for several temperatures. The data are best fitted with a logarithmic current dependence of the surface barrier  $U(I_s)$ , as seen from the straight lines obtained on a log-log scale. The temperature dependence of the slope is consistent with thermal activation with  $U_0 \sim 70$  K for  $T < 5$  K and decreasing in value for  $T > 5$  K.

The temperature dependence of the critical current for samples A and B is shown in Fig. 4. The as-measured critical currents are shown together with the bulk ( $I_{cb}$ ) and edge ( $I_{cs}$ ) contributions obtained by the procedure described above. The two samples were grown in the same batch and are expected to be similar in quality, but they differ in thickness, with sample B three times thicker than sample A. Comparing the bulk critical current densities ( $J_{cb} = I_{cb}/wd$ ) in the two samples we find that below the peak effect they are practically identical, despite the fact that the average critical current density  $J_c = I_c/wd$  calculated in the usual way as the total critical current divided by the sample cross section is more than 3 times larger in sample B than in A. These data show that the two samples are identical in their bulk pinning properties and that the distribution of pinning centers in the bulk is homogeneous. The significant difference between the bulk and average critical current densities must therefore be due to the surface barrier. Comparing the surface critical sheet current densities, defined as  $J_{cs} = I_{cs}/d$ , we find a strong enhancement of the edge critical current density in sample B compared to sample A, which implies that the surface barrier in the thicker sample is larger. More work is needed to understand the dependence of the surface barrier on sample thickness.

We next consider the peak effect region,<sup>29</sup> where both

samples exhibit a well defined enhancement in the total critical current by factors of 2.0 and 2.7 for samples A and B, respectively. The shape of the peak was previously found to depend on measurement speed and contact geometry becoming much sharper and more pronounced when the contribution from vortices entering through the edges was reduced or eliminated.<sup>24,25</sup> A similar result is obtained here by separating the edge and bulk contributions to the critical current. As shown in the inset of Fig. 4 the *bulk* peak effect consists of a 20 fold enhancement in  $I_{cb}$  [ $I_{cb}(T=5.63\text{ K})=2.9\text{ mA}$ ;  $I_{cb}(T=5.66\text{ K})=59.6\text{ mA}$ ] over a temperature range narrower than the width of the zero field superconducting transition. This remarkably sharp peak is similar to that obtained when vortex crossing of edges is eliminated by using a Corbino geometry.<sup>25</sup> In the lower part of the peak  $I_{cs}$  increases rapidly with temperature compared to its monotonic decrease below the peak. This enhancement is consistent with the edge-contamination mechanism suggested by Paltiel *et al.*<sup>24</sup> since the higher critical current of the disordered phase, injected at the sample edge in the lower part of the peak effect, leads to an additional contribution to  $I_{cs}$  over and above that due to the surface barrier. These results are also consistent with the significant sharpening of the peak effect observed in high frequency ac measurements<sup>18,19,24</sup> where edge contamination is practically eliminated.

In the above analysis we assumed that the edge contribution is unchanged by cutting the sample. As a check we cut the sample a second time and compared the bulk  $V-I$  characteristics to those before cutting. Below the peak region we

found that the  $V-J_b$  curves were unchanged within better than 10%.

#### IV. CONCLUSIONS

In conclusion, by comparing the  $V-I$  curves of samples before and after they are cut, we obtained the bulk and edge contributions to the transport current at various dissipation levels. This led to the first derivation of separate  $V-I$  curves for the bulk and the edge. Below the peak region the nonlinearity of the measured  $V-I$  curves in  $2\text{H-NbSe}_2$  is due to the edge contribution and the edge current is governed by thermally activated vortex crossing through a current dependent surface barrier. By contrast the bulk  $V-I$  characteristics are linear confirming the free flux flow model for vortex motion in the bulk. In the peak effect region the temperature dependence of the bulk critical current exhibits a very sharp peak. The edge contribution starts increasing before the bulk current does, leading to a smeared out peak in the total critical current.

#### ACKNOWLEDGMENTS

This work was supported by NSF-DMR Grant No. 97-05389 and by U.S. DOE Grant No. DE-FG02-99ER45742. EZ acknowledges support by the German-Israeli Foundation G.I.F.

- 
- <sup>1</sup>C. P. Bean and J. D. Livingston, Phys. Rev. Lett. **12**, 14 (1964).  
<sup>2</sup>E. Zeldov, A. I. Larkin, V. B. Geshkenbein, M. Konczykowski, D. Majer, B. Khaykovich, V. M. Vinokur, and H. Shtrikman, Phys. Rev. Lett. **73**, 1428 (1994).  
<sup>3</sup>M. Benkraouda and J. R. Clem, Phys. Rev. B **58**, 15 103 (1998); E. H. Brandt, *ibid.* **59**, 3369 (1999).  
<sup>4</sup>Dan T. Fuchs, Eli Zeldov, Michael Rappaport, Tsuyoshi Tamegai, Shuuichi Ooi, and Hadas Shtrikman, Nature (London) **391**, 373 (1998).  
<sup>5</sup>D. T. Fuchs, E. Zeldov, T. Tamegai, S. Ooi, M. Rappaport, and H. Shtrikman, Phys. Rev. Lett. **80**, 4971 (1998).  
<sup>6</sup>D. T. Fuchs, R. A. Doyle, E. Zeldov, S. F. W. R. Rycroft, T. Tamegai, S. Ooi, M. L. Rappaport, and Y. Myasoedov, Phys. Rev. Lett. **81**, 3944 (1998).  
<sup>7</sup>Y. Paltiel, D. T. Fuchs, E. Zeldov, Y. N. Myasoedov, H. Shtrikman, M. L. Rappaport, and E. Y. Andrei, Phys. Rev. B **58**, R14 763 (1998).  
<sup>8</sup>M. Konczykowski, L. I. Burlachkov, Y. Yeshurun, and F. Holtzberg, Phys. Rev. B **43**, 13 707 (1991).  
<sup>9</sup>N. Chikumoto, M. Konczykowski, N. Motohira, and A. P. Malozemoff, Phys. Rev. Lett. **69**, 1260 (1992).  
<sup>10</sup>L. Burlachkov, V. B. Geshkenbein, A. E. Koshelev, A. I. Larkin, and V. M. Vinokur, Phys. Rev. B **50**, 16 770 (1994).  
<sup>11</sup>L. Burlachkov, A. E. Koshelev, and V. M. Vinokur, Phys. Rev. B **54**, 6750 (1996).  
<sup>12</sup>S. F. W. R. Rycroft, R. A. Doyle, D. T. Fuchs, E. Zeldov, R. J. Drost, P. H. Kes, T. Tamegai, S. Ooi, and D. T. Foord, Phys. Rev. B **60**, R757 (1999).  
<sup>13</sup>P. K. Mishra, G. Ravikumar, T. V. C. Rao, V. C. Sahni, S. S. Banerjee, S. Ramakrishnan, A. K. Grover, and M. J. Higgins, Physica C **340**, 65 (2000).  
<sup>14</sup>M. J. Higgins and S. Bhattacharya, Physica C **257**, 232 (1996).  
<sup>15</sup>X. S. Ling, J. E. Berger, and D. E. Prober, Phys. Rev. B **57**, R3249 (1998).  
<sup>16</sup>W. Henderson, E. Y. Andrei, M. J. Higgins, and S. Bhattacharya, Phys. Rev. Lett. **77**, 2077 (1996).  
<sup>17</sup>Z. L. Xiao, E. Y. Andrei, P. Shuk, and M. Greenblatt, Phys. Rev. Lett. **85**, 3265 (2000).  
<sup>18</sup>W. Henderson, E. Y. Andrei, and M. Higgins, Phys. Rev. Lett. **81**, 2352 (1998).  
<sup>19</sup>E. Y. Andrei, Z. L. Xiao, W. Henderson, M. J. Higgins, P. Shuk, and M. Greenblatt, J. Phys. IV **10**, 5 (1999).  
<sup>20</sup>Z. L. Xiao, E. Y. Andrei, and M. J. Higgins, Phys. Rev. Lett. **83**, 1664 (1999).  
<sup>21</sup>U. Yaron, P. L. Gammel, D. A. Huse, R. N. Kleinman, C. S. Oglesby, E. Bucher, B. Batlogg, D. J. Bishop, K. Mortensen, and K. N. Clausen, Nature (London) **376**, 753 (1995).  
<sup>22</sup>F. Pardo, F. de la Cruz, P. L. Gammel, E. Bucher, and D. J. Bishop, Nature (London) **396**, 348 (1998).  
<sup>23</sup>Z. L. Xiao, E. Y. Andrei, P. Shuk, M. Greenblatt, Phys. Rev. Lett. **86**, 2431 (2001).  
<sup>24</sup>Y. Paltiel, E. Zeldov, Y. N. Myasoedov, H. Shtrikman, S. Bhattacharya, M. J. Higgins, Z. L. Xiao, E. Y. Andrei, P. L. Gammel, and D. J. Bishop, Nature (London) **403**, 398 (2000).  
<sup>25</sup>Y. Paltiel, E. Zeldov, Y. Myasoedov, M. L. Rappaport, G. Jung, S. Bhattacharya, M. J. Higgins, Z. L. Xiao, E. Y. Andrei, P. L.

- Gammel, and D. J. Bishop, Phys. Rev. Lett. **85**, 3712 (2000).
- <sup>26</sup>S. S. Banerjee, N. G. Patil, S. Saha, S. Ramakrishnan, A. K. Grover, S. Bhattacharya, G. Ravikumar, P. K. Mishra, T. V. Chandrasekhar Rao, V. C. Sahni, M. J. Higgins, E. Yamamoto, Y. Haga, M. Hedo, Y. Inada, and Y. Onuki, Phys. Rev. B **58**, 995 (1998).
- <sup>27</sup>Y. B. Kim, C. F. Hempstead, and A. R. Strnad, Phys. Rev. **139**, A1163 (1965).
- <sup>28</sup>J. Bardeen and M. J. Stephen, Phys. Rev. **140**, A1197 (1965).
- <sup>29</sup>In the peak effect region the current separation is sensitive to the position of the peak. A small shift in the peak, due for example to a misalignment between the  $c$  axis of the sample and the field, can lead to different relative magnitudes of edge and bulk contributions. In spite of these variations, we found that the peak in the bulk contribution was always significantly sharper than that in the total current.